

THE LOWEST RESONANCE IN QCD FROM LOW-ENERGY DATA

L. AMETLLER^a AND P. TALAVERA^{bc}

^a*Departament de Física i Enginyeria Nuclear, Universitat Politècnica de Catalunya,
Jordi Girona 13, E-08034 Barcelona, Spain*

^b*Departament de Física i Enginyeria Nuclear, Universitat Politècnica de Catalunya,
Comte Urgell 187, E-08036 Barcelona, Spain.*

^c*Institut de Ciències del Cosmos, Universitat de Barcelona,
Diagonal 647, E-08028 Barcelona, Spain.*

Abstract

We show that a generalization of $su(2)$ Chiral Perturbation Theory, including a perturbative singlet scalar field, converges faster towards the physical value of sensible low-energy observables. The physical mass and width of the scalar particle are obtained through a simultaneous analysis of the pion radius and the $\gamma\gamma \rightarrow \pi^0\pi^0$ cross-section. Both values are statistically consistent with the ones obtained by using Roy equations in $\pi - \pi$ scattering. In addition we find indications that the photon-photon-singlet coupling is quite small.

1 Motivation

Scalar particles are neither too well known from experiment nor their properties are theoretically understood. Having the quantum numbers of the vacuum, the lightest scalar particle, the σ , couples strongly to pions and that makes it important for all the models involving spontaneous chiral symmetry breaking.

Scalar extensions of Chiral Perturbation Theory (χ PT) have been analyzed in the past by several authors. Recently, it has been proposed to include an isosinglet scalar as a dynamical degree of freedom to the χ PT Lagrangian, [1] at the same footing as the lowest mass pseudoscalar Goldstone bosons. With this, one is trying to obtain a better description of the low-energy processes among pions and, at the same time, to describe the nature of the σ . In fact it is commonly expected that the physics of the σ would be governed by the dynamics of the Goldstone bosons, thus being the properties of the interaction between two pions relevant [2].

In this note, we look for experiments involving pions and photons at low-energy which can be—at least in principle—sensible to the dynamics of the scalar meson in order to obtain restrictions for the new couplings of the $S\chi$ PT Lagrangian. In doing so, we restrict ourselves to the scenario where the free parameters of the model will be the σ mass, M_σ , its width Γ_σ and the $\sigma\pi\pi$ coupling constants. We focus on two observables: The vector form-factor of the charged pion and the $\gamma\gamma \rightarrow \pi^0\pi^0$ cross section. The first has been measured reasonably well in the space-like region and data for the second are rather old and also poor, but nevertheless it is a process of great interest thus can enlighten about the controversial $\sigma\gamma\gamma$ coupling.

A common feature for these two processes is that, in both, the number of additional constants wrt χ PT is minimal. This is given by the fact that in the aforementioned processes neither the mass nor the decay constant are renormalized at one loop. In addition, for the $\gamma\gamma \rightarrow \pi^0\pi^0$ process not even the wave function renormalization is required. This essentially has as outcome that there is only one new coupling as relevant parameter.

2 Formalism

Our starting point is the $S\chi$ PT Lagrangian discussed in [1], an extension of the lowest order χ PT Lagrangian for Goldstone bosons with the inclusion of a scalar isosinglet. We will be concerned only with processes involving low-energy pions or photons as asymptotic states. In addition to this premise we should impose the scale hierarchy chain

$$p, M_\pi, M_\sigma \ll \Lambda_\chi. \quad (1)$$

The $S\chi$ PT Lagrangian involves pions and the S_1 scalar field—that we identify with the σ , transforming as a singlet under $SU(2)_L \times SU(2)_R$ —respects Chiral symmetry, P and C

invariance and explicitly reads at lowest order

$$\mathcal{L}_2[0^{++}] = \left(\frac{F^2}{4} + F c_{1d} S_1 + c_{2d} S_1^2 + \dots \right) \langle u_\mu^\dagger u^\mu \rangle + \left(\frac{F^2}{4} + c_{2m} S_1^2 + \dots \right) (\langle \chi_+ \rangle - \langle \chi^\dagger + \chi \rangle) . \quad (2)$$

Notice that by counting–power and gauge invariance a term involving the coupling $\gamma\gamma S_1$ is forbidden at this stage. As it stands (2) is a generalization of the Lagrangian corresponding to the singlet discussed in [3] from where we borrow part of our notation in what follows. The labels in the coupling constants c indicate the number of scalar fields coupled to pions and the derivative- or massive-type of pion coupling. Ellipsis stand for higher order terms involving higher powers of the singlet field, which are scale suppressed. Here we take into account that c_{1m} is zero, to enforce the scalar field to be a singlet under chiral symmetry and not mix with the vacuum. As is customary the field u parameterizes the pseudoscalar Goldstone bosons

$$u^2 = U = e^{i\sqrt{2}\phi/F}, \quad \phi = \begin{pmatrix} \pi^0 & \sqrt{2}\pi^+ \\ \sqrt{2}\pi^- & -\pi^0 \end{pmatrix}, \quad (3)$$

and the χ field denotes the combination $\chi = 2B_0(s + ip)$. F is the pion decay constant in the chiral limit. In the rest we have made use of the following notation

$$\begin{aligned} u_\mu &= iu^\dagger D_\mu U u^\dagger = -iu D_\mu U^\dagger u = u_\mu^\dagger, \\ \chi_\pm &= u^\dagger \chi u^\dagger \pm u \chi^\dagger u, \\ f_\pm^{\mu\nu} &= u F_L^{\mu\nu} u^\dagger \pm u^\dagger F_R^{\mu\nu} u. \end{aligned} \quad (4)$$

The quantities $F_L^{\mu\nu}$, $F_R^{\mu\nu}$ are related with the field strength associated with the non–abelian external fields.

The $O(p^2)$ Lagrangian (2) will contribute to amplitudes at $O(p^4)$ through one–loop graphs, which in turn will give rise to ultraviolet divergences. In the case at hand the cancellation of such divergences proceeds only through a single counterterm, ℓ_6^1 . In addition there can be a possible pure electromagnetic contribution in terms of a $S_1\gamma\gamma$ coupling, $c_{\gamma 1}$,

$$\mathcal{L}_4[0^{++}] = \ell_6 \frac{1}{4} i \langle f_+^{\mu\nu} [u_\mu, u_\nu] \rangle + \left(-\frac{1}{4} F_{\mu\nu} F^{\mu\nu} - \frac{\lambda}{2} (\partial_\mu A^\mu)^2 \right) (1 + c_{\gamma 1} S_1 + \dots) . \quad (5)$$

This last term has long been debated and is crucial to elucidate the composition of the scalar: non–strange $q\bar{q}$ state, $s\bar{s}$ state, tetra–quark state, $K\bar{K}$ molecule, glueball However it is practically impossible to determine experimentally this coupling at present and only a combined study of several processes could in principle disentangle its value. For practical purpose we have considered it subleading in the counting–power, $|c_{\gamma 1} c_{1d}| \leq 1/(4\pi F)^2$. Afterwards we will check the validity of this assumption through the consistency of the theoretical predictions versus the experimental results. We want to stress that this is the only point where we

¹In order to avoid confusion with the low–energy constants in χ PT the $S\chi$ PT ones are denoted by ℓ_i while the former by l_i .

add some extra assumption on top of just chiral symmetry constraints.

We have used dimensional regularization with $\omega \equiv (d-4)/2$ in the $\overline{\text{MS}}$ scheme. In this regularization the only low-energy constant we need is defined as:

$$\ell_6 = \ell_6^r + \gamma_6 \lambda, \quad (6)$$

with $\lambda = \frac{\mu^{2\omega}}{16\pi^2} \left\{ \frac{1}{2\omega} - \frac{1}{2}(\log 4\pi + \Gamma'(1) + 1) \right\}$. The ℓ_6^r is the coupling constant renormalized at the scale μ and the γ_6 factor is found via the Heat-Kernel expansion and is given by

$$\gamma_6 = \frac{1}{3}(4c_{1d}^2 - 1). \quad (7)$$

Finally the derivative of the Γ function is the Euler constant, $\Gamma'(1) = -\gamma$.

2.1 The vector form-factor of the pion

The vector form-factor of the pion is defined through the matrix element $\langle \pi^i(p') | V_\mu^k | \pi^l(p) \rangle = i\epsilon^{ikl}(p'_\mu + p_\mu)F_V(q^2)$. We have computed it at $O(p^4)$ in $S\chi\text{PT}$ and have obtained the result

$$F_V(t) = 1 + \frac{t}{96\pi^2 F^2} \left(\bar{\ell}_6 - \frac{1}{3} \right) + \frac{1}{6F^2} (t - 4M_\pi^2) \bar{J}_{\pi\pi}(t) + \frac{c_{1d}^2}{F^2} \frac{1}{(t - 4M_\pi^2)} (P_V + U_V). \quad (8)$$

The first three terms in (8) are independent of c_{1d} and correspond to the well known χPT contribution [4], provided one identifies $\bar{\ell}_6$ with \bar{l}_6 . The rest is the contribution of the scalar singlet, and is split into two terms, a polynomial piece given by

$$\begin{aligned} P_V = & -\frac{\bar{\ell}_6 t}{24\pi^2} (t - 4M_\pi^2) - 8(M_\sigma^2 - 2M_\pi^2)^2 \left[\frac{4M_\pi^4 + M_\sigma^4 - M_\pi^2(4M_\sigma^2 + t)}{(M_\pi^2 - M_\sigma^2)(4M_\pi^2 - M_\sigma^2)} \right] (\mu_\pi - \mu_\sigma) \\ & + \frac{[4M_\pi^2(14M_\pi^2 t + 72M_\pi^4 + t^2) + 18(12M_\pi^2 + t)M_\sigma^4 - (68M_\pi^2 t + 432M_\pi^4 + t^2)M_\sigma^2 - 36M_\sigma^6]}{72\pi^2(4M_\pi^2 - M_\sigma^2)}, \end{aligned} \quad (9)$$

and the dispersive part of the form-factor

$$\begin{aligned} U_V = & 4(M_\sigma^2 - 2M_\pi^2)^2 (4M_\pi^2 - 2M_\sigma^2 - t) C_0(t, M_\pi^2, M_\pi^2, M_\pi^2, M_\pi^2, M_\sigma^2) \\ & - \frac{2}{3} [t^2 + 64M_\pi^4 + 12M_\sigma^4 - 8M_\pi^2(6M_\sigma^2 + t)] \bar{J}_{\pi\pi}(t) \end{aligned} \quad (10)$$

$$- 4(M_\sigma^2 - 2M_\pi^2)^2 \left[\frac{4M_\pi^4 + tM_\sigma^2 - M_\pi^2(2M_\sigma^2 + 3t)}{M_\pi^2(4M_\pi^2 - M_\sigma^2)} \right] \bar{J}_{\pi\sigma}(M_\pi^2). \quad (11)$$

The $C_0(q^2, M_\pi^2, M_\pi^2, M_\pi^2, M_\pi^2, M_\sigma^2)$ function stands for the one-loop scalar three-point function [5], and $\bar{J}_{ab}(q^2)$ and μ_a are the one-loop scalar two-point and one-point function, subtracted at $q^2 = 0$, respectively [4]. The last term in (8) apparently contains a pole at $t = 4M_\pi^2$, but we have checked numerically that it is spurious. Moreover, we have also checked numerically that, at zero momentum transfer, the form-factor fulfills the expecta-

tions from the Ademollo–Gatto theorem [6]: $F_V(0^-) = 1$. Notice that the above expression displays t^2 dependences that are customary of $O(p^6)$ in χ PT. That is the reason we believe that $S\chi$ PT can achieve a better convergence than χ PT at moderate energies.

2.2 The $\gamma\gamma \rightarrow \pi^0\pi^0$ amplitude

It is well known that the lowest order contribution to this process in χ PT is a pure $O(p^4)$ loop effect, which is finite by itself without any need of counterterms. This makes this process a gold plated test of χ PT. However, when comparing the one loop prediction with existing experimental data, even near threshold, they differ significantly [7, 8]. In order to improve the agreement, one is forced to work at two-loop order [9] or to rely on a dispersive treatment [10]. We expect that the simple inclusion of the scalar particle would interpolate between both outcomes and ameliorate the situation at relatively higher energies, $\approx 0.6 - 0.7$ GeV.

We have computed the $\gamma\gamma \rightarrow \pi^0\pi^0$ amplitude in $S\chi$ PT assuming the mass scale hierarchy previously mentioned, where the direct $S_1\gamma\gamma$ coupling is negligible. This switches-off tree contributions and the process is driven entirely by loops making the comparison with χ PT at the same footing.

The amplitude at $O(p^4)$ is purely S-wave and can be written as

$$A(s) = \frac{4e^2}{F^2} \frac{(s - M_\pi^2)}{s} [1 + F_\sigma(s)] \overline{G}(s) \left(\frac{1}{2} s \epsilon_1 \cdot \epsilon_2 - q_1 \cdot \epsilon_2 q_2 \cdot \epsilon_1 \right), \quad (12)$$

where q_i, ϵ_i , are the photon momenta, polarizations respectively and $s = (q_1 + q_2)^2$. We have collected the effects of the scalar singlet inside the factor

$$F_\sigma(s) = -4c_{1d}^2 \frac{(s - 2M_\pi^2)^2}{(s - M_\pi^2)} \frac{1}{s - s_0}, \quad s_0^{1/2} \equiv M_\sigma \quad (13)$$

and finally the function $\overline{G}(s)$ is given in Eqs.(C1-C5) of Ref. [9]. Notice that we obtain a finite $O(p^4)$ amplitude.

For convenience when comparing with experimental results we will make use of the cross-section

$$\sigma(\gamma\gamma \rightarrow \pi^0\pi^0) = Z \frac{\alpha^2 \pi}{F^4} \frac{(s - M_\pi^2)^2}{s} \beta(s, M_\pi^2) |1 + F_\sigma(s)|^2 |\overline{G}(s)|^2, \quad \beta(s, M_\pi^2) = (1 - 4M_\pi^2/s)^{1/2} \quad (14)$$

where Z is a factor that parameterizes the angular range of the experiment, $Z = \cos(\theta_{\max})$.

The most problematic feature involved in the previous expression (12) is that it does not comply with unitarity. In fact, there appears a pole at $s = s_0$. In order to amend this drawback we regularize the real part by changing the above delta distribution by a Breit–Wigner,

$$s_0^{1/2} \rightarrow M_\sigma - i\Gamma'. \quad (15)$$

Even though the use of the Breit-Wigner distribution seems a bit controversial in our framework where $\Gamma' \gg M_\sigma$ [11, 12].

There is substantial phenomenological evidence, [13], that Γ' *can not* be interpreted as given directly in terms of the squared coupling constant. This would only be valid for a narrow resonance in a region where the background is negligible. To circumvent this problem we consider Γ' as a phenomenological free parameter, at first instance unrelated to c_{1d} , checking afterwards the consistency of this picture.

3 Numerical results

In order to estimate the optimal values of the unknown parameters we have used a Monte-Carlo approach and fitted the available data on the space-like pion form-factor and on the $\gamma\gamma \rightarrow \pi^0\pi^0$ process to the corresponding theoretical expressions (8), (14).

Data for the $\gamma\gamma \rightarrow \pi^0\pi^0$ process are very scarce, relatively old and with very large uncertainties. We used a subset of the Cristall Ball data [14] restricted to energies up to ≈ 0.75 GeV, where we expect our effective approach should still be valid.

For the pion form-factor we entirely rely on the space-like region data [15, 16], but we have cross-checked that including the more fuzzy time-like data our findings are statistically consistent with the results we present below. When analyzed within χ PT the two space-like data sets show a small inconsistency [17] that turns to be negligible for the sensitivity of our analysis. The main reasons for focusing in the space-like region are: *i*) the data set is large enough to evade some significant statistical fluke and *ii*) the errors are rather small in comparison with available data in the time-like region. As mentioned earlier the aim to include these data is to impose severe constraints on c_{1d} . In [1] this constant was obtained from the decay width of the scalar by assuming that the latter is obtained from Roy equations for the isoscalar S-wave $\pi\pi$ scattering amplitude near threshold [2].

The fitting strategy is as follows: we have randomly sampled with 2×10^6 configurations the set of parameters $\{m_\sigma, \Gamma, \bar{\ell}_6, c_{1d}\}$ in the hypercube

$$0.3 \text{ GeV} \leq M_\sigma \leq 0.7 \text{ GeV}, \quad 0 \text{ GeV} \leq \Gamma' \leq 0.6 \text{ GeV}, \quad 10 \leq \bar{\ell}_6 \leq 30, \quad 0.1 \leq c_{1d} \leq 0.5, \quad (16)$$

with a priori flat distribution. The extremal values accommodate any reasonable outcome for those constants. The most favorable set of values is obtained by minimizing a χ^2 distribution. As numerical inputs we used the pion physical masses and decay constant

$$M_{\pi^0} = 134.9766 \text{ MeV}, \quad M_{\pi^+} = 139.57 \text{ MeV}, \quad F_\pi = 93 \text{ MeV}. \quad (17)$$

Before presenting the full analysis we perform individual fits for both processes with the result,

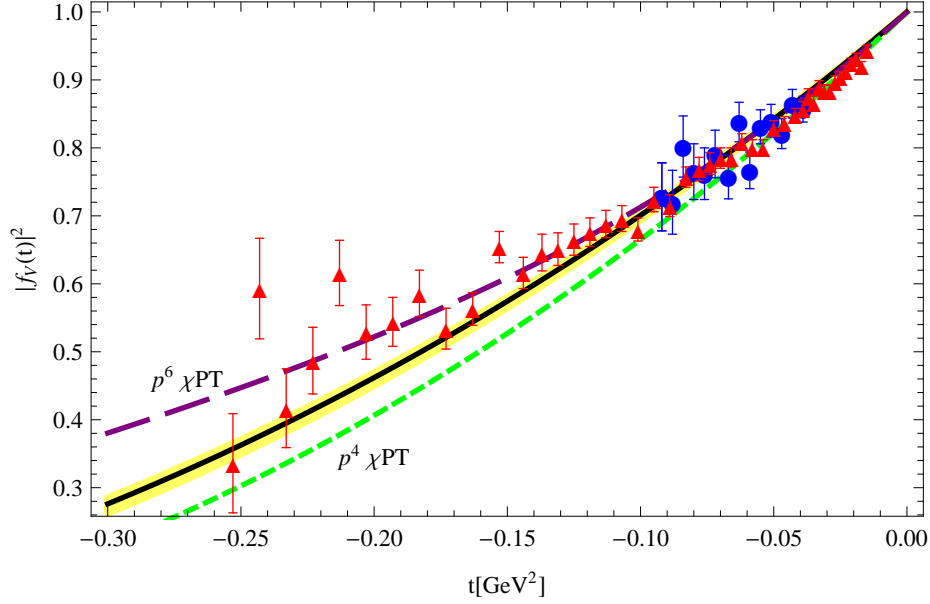


Figure 1: Pion form-factor: Full line is obtained evaluating (8) at the central values of the parameters in (21). For comparison we plot the χ PT result at $O(p^4)$, short-dashed line, with $\bar{l}_6 = 16.5$ [4]. If we decrease this value down to ≈ 15 both curves, full and dashed, agree. The band covers the 1σ uncertainty around the values in (21). The long-dashed line is the χ PT result at $O(p^6)$ and is shown for completeness.

1. $\pi \rightarrow \pi\gamma$

$$c_{1d} = 0.10, \quad M_\sigma = 697 \text{ MeV}, \quad \bar{l}_6 = 15.33, \quad (18)$$

2. $\gamma\gamma \rightarrow \pi^0\pi^0$

$$c_{1d} = 0.49, \quad M_\sigma = 413 \text{ MeV}, \quad \Gamma' = 399 \text{ MeV}. \quad (19)$$

The outcome is rather pedagogical: as the physics of the pion form-factor is already well understood in terms of vector saturation, the scalar contribution, if any, must be tiny. This is reflected in the small value of c_{1d} . Contrariwise, as the $\gamma\gamma\pi^0\pi^0$ cross-section is very poorly understood in terms of pion rescattering effects this allows some room to incorporate the contribution of the scalar particle. We expect that the combined analysis maximizes the possible effect of the scalar particle in the $\gamma\gamma\pi^0\pi^0$ reaction while we keep the common parameters under control due to the restrictions imposed by the pion form-factor.

The combined simultaneous fit is performed by minimizing an augmented χ^2 distribution

$$\chi^2 = \chi_{FV}^2 + \chi_{\gamma\gamma \rightarrow \pi^0\pi^0}^2, \quad (20)$$

where both sets of experiments are weighted equally. The landscape contains a single mini-

imum for the χ^2 function corresponding to

$$c_{1d} = 0.22^{+0.13}_{-0.06}, \quad \bar{\ell}_6 = 18.03^{+10.39}_{-1.86}, \quad M_\sigma = 497^{+44}_{-64} \text{ MeV}, \quad \Gamma' = 233^{+291}_{-117} \text{ MeV}, \quad \chi^2_{d.o.f} = \frac{162.7}{65}. \quad (21)$$

The errors capture the deviation within 1σ of the central result, i.e., we keep configuration points fulfilling $\chi^2 < \chi^2_{4,0.6827}$, where the upper bound corresponds to a probability of 68.27% for the 4 fitted parameters [18]. We have checked that, ballpark, any other point in a reasonable vicinity of (21) leads to similar results.

In fig.(1) and fig.(3) we have plotted, full line, the solution corresponding to the central parameters (21) together with the set of parameters that deviate from the former at most 1σ , yellow band. For comparison purposes we also depicted the χ PT results in dashed lines, see fig.(2). As one could anticipate the impact on the pion form-factor is almost imperceptible while the extra parameters wrt the χ pt framework fairly accommodate the $\gamma\gamma \rightarrow \pi^0\pi^0$ experimental data. It is worth noticing that the outcome of S χ PT interpolates between $O(p^4)$ and $O(p^6)$ results of standard χ PT.

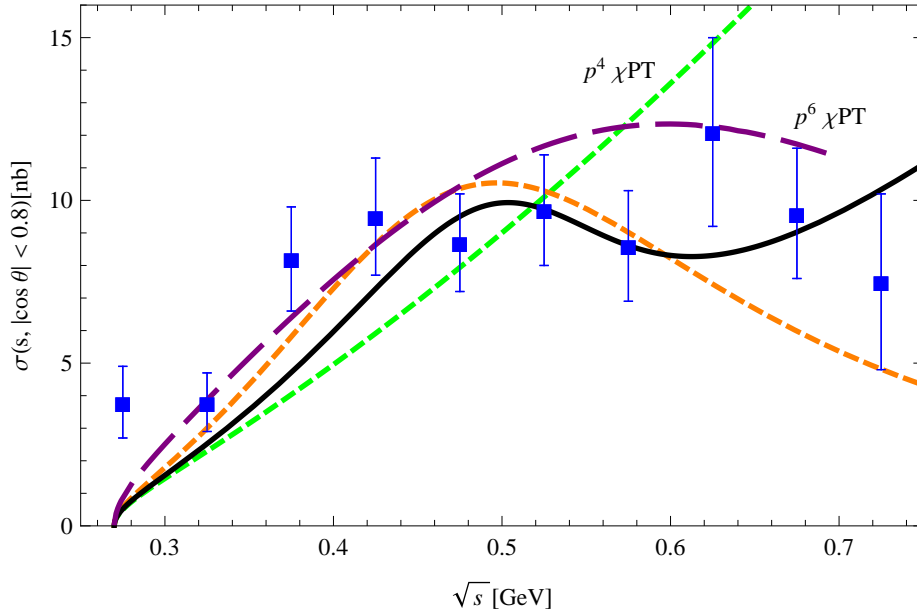


Figure 2: Cross-section for $\gamma\gamma \rightarrow \pi^0\pi^0$ integrated over $|\cos\theta^*| < 0.8$ as a function of the $\pi\pi$ invariant mass $M_{\pi\pi}$: Full line is obtained evaluating (12) at (21). The green short-dashed line is the $O(p^4)$ χ PT prediction [7] which does not depend on any low-energy constant. The long-dashed is the $O(p^6)$ χ PT result in [19]. The orange short-dashed curve shows the best fit performed using the data of this channel alone (19).

3.1 Comparison with earlier results

Part of the outputs in (21), M_σ and Γ' , can be compared to earlier results, see table 1.

| | [2] | [20] | [21] | [22] | [23] | [24] |
|------------------|-------------------|--------------|--------------|-------------------|--------------|--------------|
| M_σ [MeV] | 441^{+16}_{-8} | 478 ± 29 | 541 ± 29 | 457^{+14}_{-13} | 470 ± 50 | 434 ± 78 |
| Γ [MeV] | 544^{+18}_{-26} | 324 ± 22 | 504 ± 84 | 558^{+22}_{-14} | 570 ± 50 | 404 ± 86 |

Table 1: Comparison with some results in the literature.

While the agreement between masses is quite encouraging there is a mismatch between the central values for the widths that roughly amounts to a factor 2, with the exception of the data on $D \rightarrow \pi^+ \pi^- \pi^+$ of E791 [20]. In order to understand and quantify this disagreement, we fix the mass and the width of the S_1 to the central values given in [2] and redo the analysis with the following outcome

$$c_{1d} = 0.26^{+0.005}_{-0.027}, \quad \bar{\ell}_6 = 19.98^{+0.01}_{-1.32}, \quad \chi^2_{d.o.f} = \frac{168.82}{67}, \quad (22)$$

i.e. the central values of both c_{1d} ($\bar{\ell}_6$) change by less than 20% (10%) with respect to the values in (21). Furthermore both results are statistically equivalent, notice that the narrow pink band in fig.(3) corresponding to the uncertainties on the central value of (22) is contained in the wider band corresponding to the 1σ values of (21) while the deviation in the pion form-factor is still within the 1σ band in fig.(1). In view of the previous result one can conclude that, with the present data on $\gamma\gamma\pi^0\pi^0$, our results for the mass and width of the scalar field (21) are compatible with that in [2].

The value of the constant c_{1d} must be compared with that obtained in [1], $c_{1d} = 0.67$, where lattice data were used and, more important, the coupling was essentially deduced from the scalar decay width. In the present analysis this constant turns out to be a factor 3 smaller. As mentioned above the assumption that the physical width and coupling constant of the vertex $\sigma\pi\pi$ are related by a simple dispersion relation is probably too naive. Even though one should bear in mind that, as is evident from the form of (8), there must be a strong linear correlation between the pair $\{c_{1d}^2, \bar{\ell}_6\}$.

To evaluate this statement quantitatively we have evaluated the correlation matrix between the different pairs of variables

$$\begin{matrix} c_{1d}^2 & \bar{\ell}_6 & M_\sigma^2 & \Gamma' \\ c_{1d}^2 & \bar{\ell}_6 & M_\sigma^2 & \Gamma' \end{matrix} \begin{pmatrix} 1 & 0.97 & -0.26 & 0.72 \\ 0.97 & 1 & -0.24 & 0.68 \\ -0.26 & -0.24 & 1 & -0.3 \\ 0.72 & 0.68 & -0.3 & 1 \end{pmatrix}. \quad (23)$$

As a consequence one can increase the value of c_{1d} by increasing $\bar{\ell}_6$ but, nevertheless, the value obtained in [1] for c_{1d} is so big that its corresponding $\bar{\ell}_6$ implied for (23) is presumably ruled out by some direct measurement of the pion radii.

Finally, the value of $\bar{\ell}_6$ in (21) can be crosschecked with the two-loop one obtained in [17] $\bar{\ell}_6 = 16 \pm 0.5 \pm 0.7$.

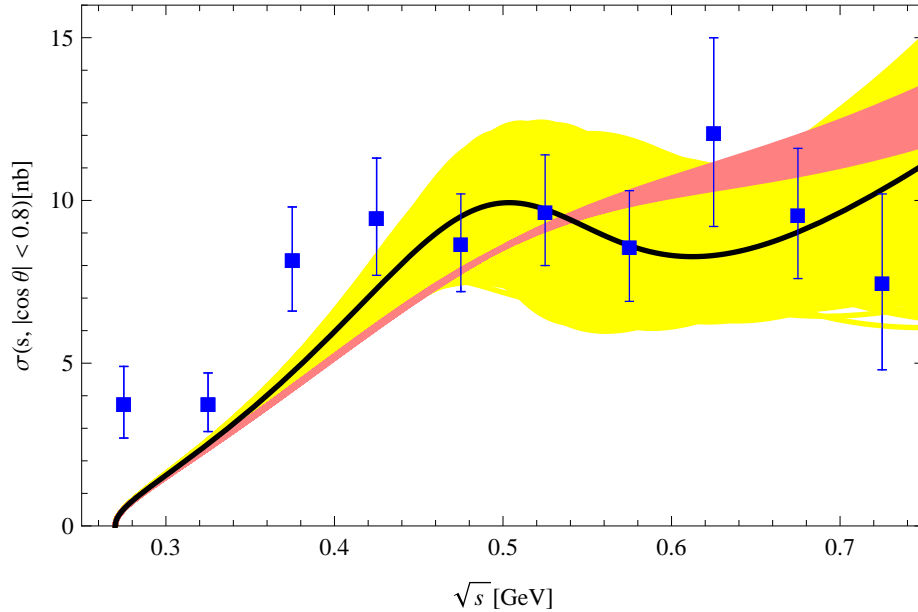


Figure 3: Cross-section for $\gamma\gamma \rightarrow \pi^0\pi^0$ integrated over $|\cos\theta^*| < 0.8$ as a function of the $\pi\pi$ invariant mass $M_{\pi\pi}$: Full line is obtained evaluating (12) at the parameters (21) and its 1σ deviation is covered by the wider, yellow, band. The narrow pink band covers the 1σ deviation of (23).

4 A sample of applications

Once our main results are obtained, we discuss their implications in a sample of applications. From one side, the dynamical scalar will contribute to some pion properties, such as the neutral pion scattering lengths and pion polarizabilities. On the other side, the σ itself gets effective radiative couplings at one loop that translate in a non vanishing $\sigma \rightarrow \gamma\gamma$ decay.

4.1 $\pi\pi$ scattering lengths

The picture for the $\pi\pi$ scattering lengths which emerges out of our low-energy Lagrangian results in a new contribution to the Current Algebra (CA), coming from the scalar in the s -channel at tree-level, and proportional to c_{1d} . Provided this is tiny we expect no huge

departures from CA. It explicitly reads

$$a_0^0 = \frac{M_\pi^2}{32\pi F^2} \left[7 + 16c_{1d}^2 \left(3 \frac{M_\pi^2}{M_\sigma^2 - 4M_\pi^2} + 2 \frac{M_\pi^2}{M_\sigma^2} \right) \right], \quad (24)$$

$$a_0^2 = \frac{M_\pi^2}{16\pi F^2} \left(-1 + 16c_{1d}^2 \frac{M_\pi^2}{M_\sigma^2} \right), \quad (25)$$

whose values are collected in the table 2.

| | CA | S χ PT | $O(p^4)\chi$ PT | Ex.(stat)(syst) |
|---------|--------|----------------------------|-----------------|-----------------|
| a_0^0 | 0.158 | $0.168^{+0.015}_{-0.007}$ | 0.2 | 0.2210(47)(40) |
| a_0^2 | -0.045 | $-0.042^{+0.005}_{-0.001}$ | - 0.042 | -0.0429(44)(28) |

Table 2: Comparison for the scattering-lengths.

As one can appreciate the S χ PT results nicely interpolate once more between two consecutive χ PT order results. We have checked that all values within the 1σ deviation for the scattering lengths in the above table are inside the universal band as defined in [25].

4.2 Neutral pion polarizabilities

To obtain the pion polarizabilities we consider the crossed channel $\gamma\pi^0 \rightarrow \gamma\pi^0$ at threshold. In our case, see (12), the electric ($\bar{\alpha}_{\pi^0}$) and magnetic ($\bar{\beta}_{\pi^0}$) polarizabilities are identical to each other. Introducing a 4π factor to conform the experimental data we obtain

$$\bar{\alpha}_{\pi^0} - \bar{\beta}_{\pi^0} = -\frac{\alpha}{3\pi^2 F^2 M_{\pi^0}} \left| \frac{1}{16} - c_{1d}^2 \frac{M_{\pi^0}^2}{M_\sigma^2 - iM_\sigma \Gamma'} \right| = (-1.01 + 0.03 \pm 0.001) \times 10^{-4} \text{fm}^3, \quad (26)$$

where the first quantity is the χ PT contribution, the second is the scalar contribution and the errors are the maximum and minimum deviation inside the 1σ values of (21). The previous result must be compared with the experimental one $(\alpha_{\pi^0} - \beta_{\pi^0})^{\text{exp}} = -1.1 \pm 1.7$ [26]. Moreover the correction due to the scalar particle in (26) is roughly a factor 20 smaller than the two-loop expression [9] meaning that the polarizabilities measurements by themselves neither would verify the existence of the scalar particle nor determine its characteristics.

4.3 S_1 radiative width

As far as the scalar particle is concerned, although we have explicitly suppressed its direct coupling to photons at leading order, our scheme allows a dynamically generated $\gamma\gamma S_1$ interaction, via pion loops at $O(p^4)$. In this context one obtains

$$\Gamma_{S_1 \rightarrow \gamma\gamma} = 16\pi\alpha^2 \frac{c_{1d}^2 (M_\sigma^2 - 2M_\pi^2)^2}{F^2 M_\sigma} |\bar{G}(M_\sigma^2)|^2 = 0.11 \text{ KeV}. \quad (27)$$

This result lies somewhat below the lower edge of the range $[0.22, 4.4]$ KeV that is available in the literature, see Table 1 in [27]. Even-though we expect at this stage that a direct $S_1\gamma\gamma$ coupling terms coming from (5) would give contributions numerically of the same order as those in (27). In view of the previous numerical result it seems hard to reconcile the picture of the singlet with a simple $u\bar{u}, d\bar{d}$ composition as found in [28].

4.4 Hadronic contribution to Muon ($g - 2$) and to $\alpha(M_Z^2)$

We reevaluate the hadronic contribution to the running of the QED fine structure constant $\alpha(s)$ at $s = M_Z^2$ and the contribution from hadronic vacuum polarization. Using analyticity and unitarity of the vacuum polarization correlator both contributions can be calculated via dispersion integrals

$$a_\mu^{\text{had}} = \frac{\alpha_{QED}^2}{3\pi^2} \int_{4M_\pi^2}^{\infty} \frac{ds}{s} R(s) K(s) \quad [29],$$

$$\Delta\alpha(M_Z^2) = -\frac{\alpha_{QED}}{3\pi} M_Z^2 \text{Re} \int_{4M_\pi^2}^{\infty} ds \frac{R(s)}{s(s - M_Z^2 - i\epsilon)} \quad [30], \quad (28)$$

where $K(s)$ is the QED kernel [31]. In turn both magnitudes are related via dispersion relation to the hadronic production rate in e^+e^- annihilation. Assuming that the main contribution of the latter at low-energies is given entirely by the pion contribution, one obtains

$$R(s) = \frac{\sigma(e^+e^- \rightarrow \text{hadrons})}{\sigma(e^+e^- \rightarrow \mu^+\mu^-)} \approx \frac{1}{4} \beta(s, M_\pi^2)^3 |F_V(s)|^2. \quad (29)$$

Obviously the main contribution to F_V is dominated by the $\rho(770)$ but at energies below 500 MeV there is a considerable fraction coming from the scalar resonance that can compete with the $\rho(770)$ tail. Inserting (8) in F_V above the contributions to both quantities as a function of the cutoff Λ are given in table 3. Once more the results including the singlet effects interpolate between two consecutive chiral orders. Those results must be compared

| $\Lambda(\text{GeV})$ | $10^{-10} \times a_\mu^{\text{had}}$ | | | $10^{-4} \times \Delta\alpha(M_Z^2)$ | | |
|-----------------------|--------------------------------------|------------|--------------------|--------------------------------------|------------|--------------------|
| | $p^4 \chi PT$ | $S\chi PT$ | $p^6 \chi PT$ [17] | $p^4 \chi PT$ | $S\chi PT$ | $p^6 \chi PT$ [17] |
| 0.32 | 2.12 | 2.26 | 2.38 | 0.035 | 0.037 | 0.039 |
| 0.35 | 6.48 | 6.92 | 7.4 | 0.117 | 0.125 | 0.13 |
| 0.40 | 16.76 | 18.11 | 20.0 | 0.350 | 0.379 | 0.42 |
| 0.45 | 28.62 | 31.25 | 35.7 | 0.679 | 0.744 | 0.86 |
| 0.50 | 40.72 | 44.92 | 53.6 | 1.084 | 1.200 | 1.45 |

Table 3: a_μ^{had} and $\Delta\alpha(M_Z^2)$ as a function of the cutt-off Λ .

with the experimental results $a_\mu^{\text{had}} = (695.1 \pm 7.5) \times 10^{-10}$, $\Delta\alpha(M_Z^2) = (277.8 \pm 2.6) \times 10^{-4}$

[32]. Notice that at $\Lambda = 0.5$ GeV the difference between the $O(p^4)$ χPT and $S\chi PT$ in both quantities roughly amounts to half the experimental error.

4.5 Pion radii

We can now expand the form factor (8) for $t \ll 4M_\pi^2$ and obtain the expression

$$F_V = 1 + \frac{1}{6} \langle r^2 \rangle_V^\pi t + \dots \quad (30)$$

where the pion charge radius is given by the linear terms as

$$\begin{aligned} \langle r^2 \rangle_V^\pi = & \frac{1}{16\pi^2 F^2} (\bar{\ell}_6 - 1) - 3 \frac{c_{1d}^2}{F^2} \left[\frac{1}{48\pi^2} \frac{M_\sigma^2}{M_\pi^4} (M_\sigma^2 - 4M_\pi^2) + \frac{1}{12\pi^2} \bar{\ell}_6 \right. \\ & + \frac{(M_\sigma^2 - 2M_\pi^2)^2}{M_\pi^4} \left\{ \frac{M_\sigma^2}{(M_\pi^2 - M_\sigma^2)} (\mu_\pi - \mu_\sigma) + \bar{J}_{\pi\sigma}(M_\pi^2) - M_\sigma^2 C_0(t, M_\pi^2, M_\pi^2, M_\pi^2, M_\pi^2, M_\sigma^2) \right. \\ & \left. \left. - 4M_\pi^4 (M_\sigma^2 - 2M_\pi^2) \partial_t C_0(t, M_\pi^2, M_\pi^2, M_\pi^2, M_\pi^2, M_\sigma^2) \right\} \Big|_{t \rightarrow 0^+} \right]. \end{aligned} \quad (31)$$

We refrain of evaluating the previous expression numerically because it contains instabilities in the kinetic range it is defined.

5 Final remarks

We have considered χPT enlarged with the inclusion of a scalar particle as a dynamical degree of freedom. By fitting experimental data on the vector form-factor of the pion and on the $\gamma\gamma \rightarrow \pi^0\pi^0$ cross-section, we have extracted the favoured values for the $S_1\pi\pi$ coupling constant, the mass and width of the scalar particle and a low-energy constant $\bar{\ell}_6$ finding that for the mass and decay width the results are statistically equivalent to those extracted with high-energy data. We have analyzed and computed the effects of this particle on a wide set of data and have found that they are somewhere in between the predictions of two consecutive orders in χPT , what makes the framework a useful extension in parameter range of the predictions of χPT .

5.1 Acknowledgments

We are grateful to J. Bijnens, J. Gasser and M. Ivanov for providing the data for the two-loop curves in our figures and to Ll. Garrido for discussion about some statistics issues.

PT gratefully acknowledges support from FPA2010-20807, 2009SGR502 and Consolider grant CSD2007-00042 (CPAN).

References

- [1] J. Soto, P. Talavera and J. Tarrus, “Chiral Effective Theory with A Light Scalar and Lattice QCD,” Nucl. Phys. B **866** (2013) 270 [arXiv:1110.6156 [hep-ph]].
- [2] I. Caprini, G. Colangelo and H. Leutwyler, “Mass and width of the lowest resonance in QCD,” Phys. Rev. Lett. **96**, 132001 (2006) [hep-ph/0512364].
- [3] G. Ecker, J. Gasser, A. Pich and E. de Rafael, “The Role of Resonances in Chiral Perturbation Theory,” Nucl. Phys. B **321** (1989) 311.
- [4] J. Gasser and H. Leutwyler, “Chiral Perturbation Theory to One Loop,” Annals Phys. **158**, 142 (1984).
- [5] G. Passarino and M. J. G. Veltman, “One Loop Corrections for $e^+ e^-$ Annihilation Into $\mu^+ \mu^-$ in the Weinberg Model,” Nucl. Phys. B **160** (1979) 151.
- [6] M. Ademollo and R. Gatto, “Nonrenormalization Theorem for the Strangeness Violating Vector Currents,” Phys. Rev. Lett. **13** (1964) 264.
- [7] J. F. Donoghue, B. R. Holstein and Y. C. Lin, “The Reaction $\gamma \gamma \rightarrow \pi^0 \pi^0$ and Chiral Loops,” Phys. Rev. D **37** (1988) 2423.
- [8] J. Bijnens and F. Cornet, “Two Pion Production in Photon-Photon Collisions,” Nucl. Phys. B **296** (1988) 557.
- [9] S. Bellucci, J. Gasser and M. E. Sainio, “Low-energy photon-photon collisions to two loop order,” Nucl. Phys. B **423** (1994) 80 [Erratum-ibid. B **431** (1994) 413] [hep-ph/9401206].
- [10] D. Morgan and M. R. Pennington, “Is low-energy $\gamma \gamma \rightarrow \pi^0 \pi^0$ predictable?,” Phys. Lett. B **272** (1991) 134.
- [11] N. G. Kelkar and M. Nowakowski, “No classical limit of quantum decay for broad states,” J. Phys. A **43**, 385308 (2010) [arXiv:1008.3917 [quant-ph]].
- [12] M. R. Pennington, “Riddle of the scalars: Where is the sigma?,” In *Frascati 1999, Hadron spectroscopy* 95-114 [hep-ph/9905241].
- [13] F. Sannino and J. Schechter, “Exploring $\pi \pi$ scattering in the $1/N(c)$ picture,” Phys. Rev. D **52**, 96 (1995) [hep-ph/9501417].
- [14] H. Marsiske *et al.* [Crystal Ball Collaboration], “A Measurement of $\pi^0 \pi^0$ Production in Two Photon Collisions,” Phys. Rev. D **41**, 3324 (1990).

- [15] E. B. Dally, J. M. Hauptman, J. Kubic, D. H. Stork, A. B. Watson, Z. Guzik, T. S. Nigmanov and V. D. Ryabtsov *et al.*, “Elastic Scattering Measurement of the Negative Pion Radius,” *Phys. Rev. Lett.* **48**, 375 (1982).
- [16] S. R. Amendolia *et al.* [NA7 Collaboration], “A Measurement of the Space - Like Pion Electromagnetic Form-Factor,” *Nucl. Phys. B* **277**, 168 (1986).
- [17] J. Bijnens, G. Colangelo and P. Talavera, “The Vector and scalar form-factors of the pion to two loops,” *JHEP* **9805**, 014 (1998) [hep-ph/9805389].
- [18] *For a nice and pedagogical exposition see for instance:*
<http://vuko.web.cern.ch/vuko/teaching/stat09/Hypothesis.pdf>
- [19] J. Gasser, M. A. Ivanov and M. E. Sainio, “Revisiting $\gamma\gamma \rightarrow \pi^+\pi^-$ at low energies,” *Nucl. Phys. B* **745** (2006) 84 [hep-ph/0602234].
- [20] E. M. Aitala *et al.* [E791 Collaboration], “Experimental evidence for a light and broad scalar resonance in $D^+ \rightarrow \pi^- \pi^+ \pi^+$ decay,” *Phys. Rev. Lett.* **86** (2001) 770 [hep-ex/0007028].
- [21] M. Ablikim *et al.* [BES Collaboration], “The sigma pole in $J/\psi \rightarrow \omega \pi^+ \pi^-$,” *Phys. Lett. B* **598** (2004) 149 [hep-ex/0406038].
- [22] R. Garcia-Martin, R. Kaminski, J. R. Pelaez and J. Ruiz de Elvira, “Precise determination of the $f_0(600)$ and $f_0(980)$ pole parameters from a dispersive data analysis,” *Phys. Rev. Lett.* **107** (2011) 072001 [arXiv:1107.1635 [hep-ph]].
- [23] Z. Y. Zhou, G. Y. Qin, P. Zhang, Z. Xiao, H. Q. Zheng and N. Wu, “The Pole structure of the unitary, crossing symmetric low energy $\pi\pi$ scattering amplitudes,” *JHEP* **0502** (2005) 043 [hep-ph/0406271].
- [24] J. -Z. Bai *et al.* [BES Collaboration], “Evidence of sigma particle in $J/\psi \rightarrow \omega \pi^+ \pi^-$,” *High Energy Phys. Nucl. Phys.* **28** (2004) 215 [hep-ex/0404016].
- [25] B. Ananthanarayan, G. Colangelo, J. Gasser and H. Leutwyler, “Roy equation analysis of $\pi\pi$ scattering,” *Phys. Rept.* **353** (2001) 207 [hep-ph/0005297].
- [26] A. E. Kaloshin and V. V. Serebryakov, “ π^+ and π^0 polarizabilities from $\gamma\gamma \rightarrow \pi\pi$ data on the base of S matrix approach,” *Z. Phys. C* **64**, 689 (1994) [hep-ph/9306224].
- [27] M. R. Pennington, “Location, correlation, radiation: Where is the sigma, what is its structure and what is its coupling to photons?,” *Mod. Phys. Lett. A* **22** (2007) 1439 [arXiv:0705.3314 [hep-ph]].

- [28] M. R. Pennington, “Sigma coupling to photons: Hidden scalar in $\gamma\gamma \rightarrow \pi^0\pi^0$,” *Phys. Rev. Lett.* **97** (2006) 011601.
- [29] N. Cabbibo and R. Gatto, “Pion Form Factors from Possible High-Energy Electron-Positron Experiments,” *Phys. Rev. Lett.* **4** (1960) 313
- [30] M. Gourdin and E. De Rafael, “Hadronic contributions to the muon g-factor,” *Nucl. Phys. B* **10** (1969) 667.
- [31] S. Eidelman and F. Jegerlehner, “Hadronic contributions to g-2 of the leptons and to the effective fine structure constant $\alpha(M_Z^2)$,” *Z. Phys. C* **67** (1995) 585 [hep-ph/9502298].
- [32] M. Davier and A. Hocker, “Improved determination of $\alpha(M_Z^2)$ and the anomalous magnetic moment of the muon,” *Phys. Lett. B* **419** (1998) 419 [hep-ph/9711308].